Supplementary Figure 1

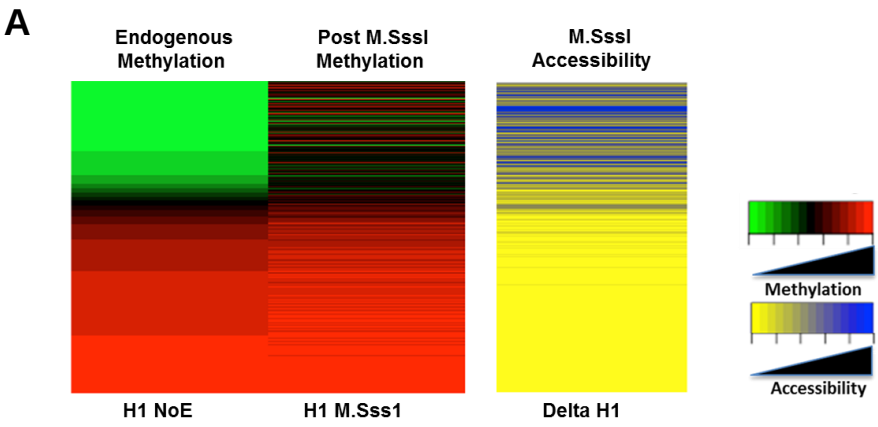

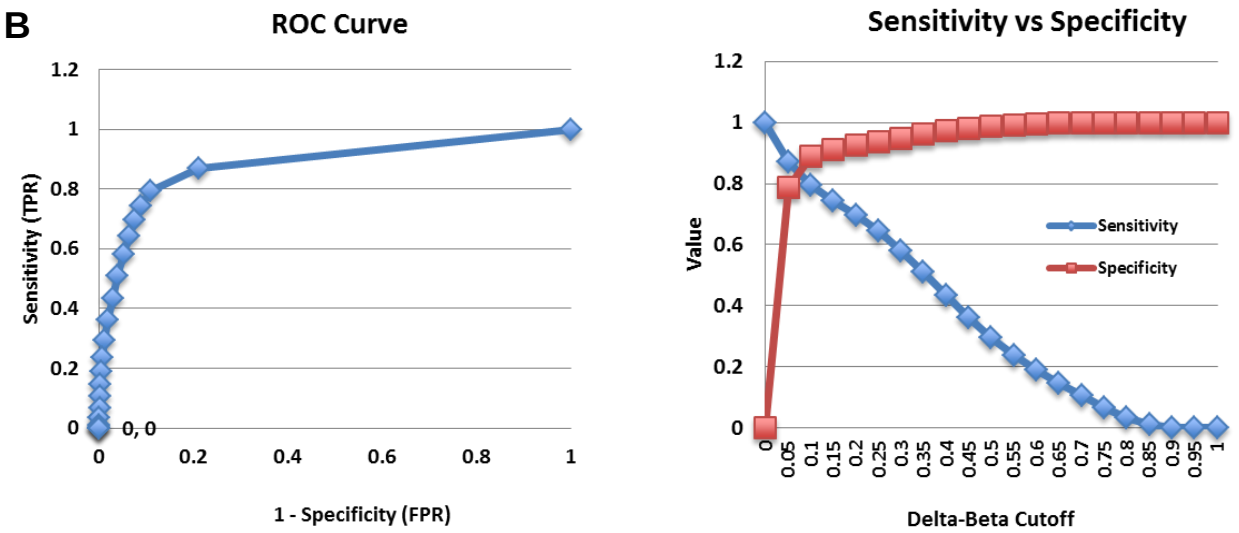

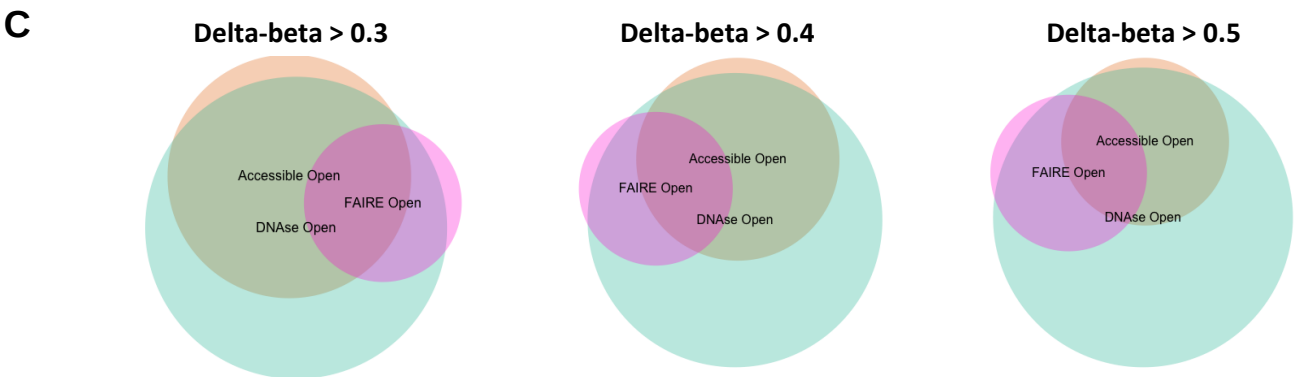

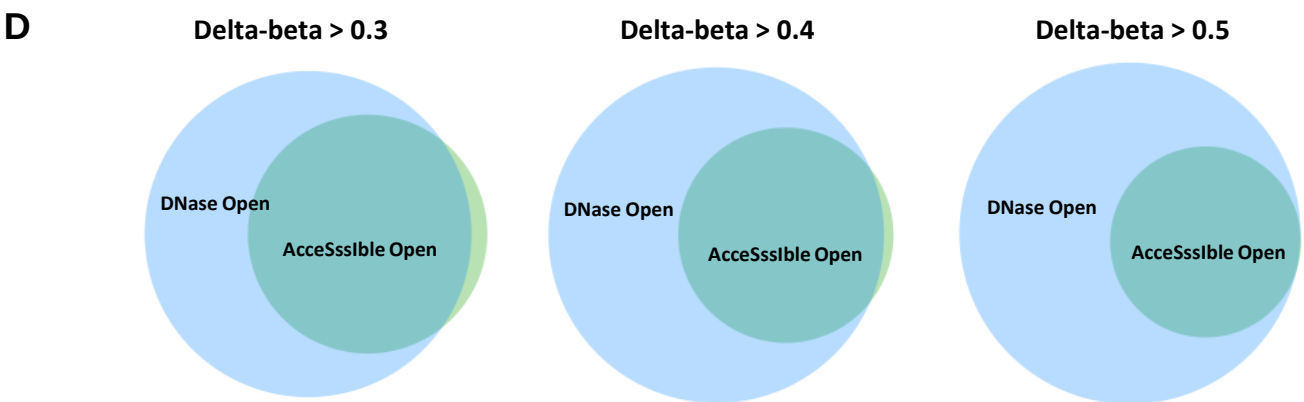

Supplementary Figure 2

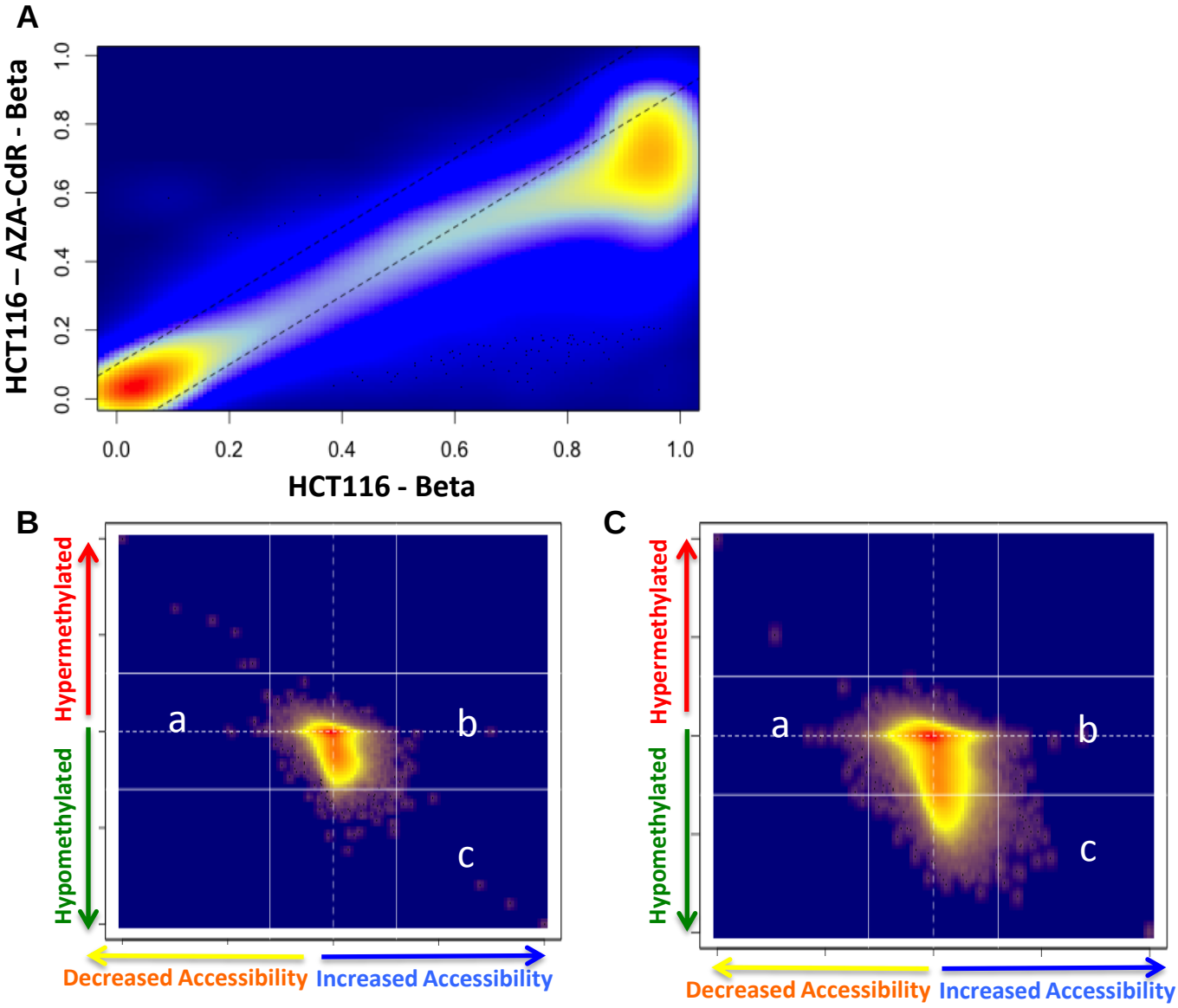

Supplementary Figure 3

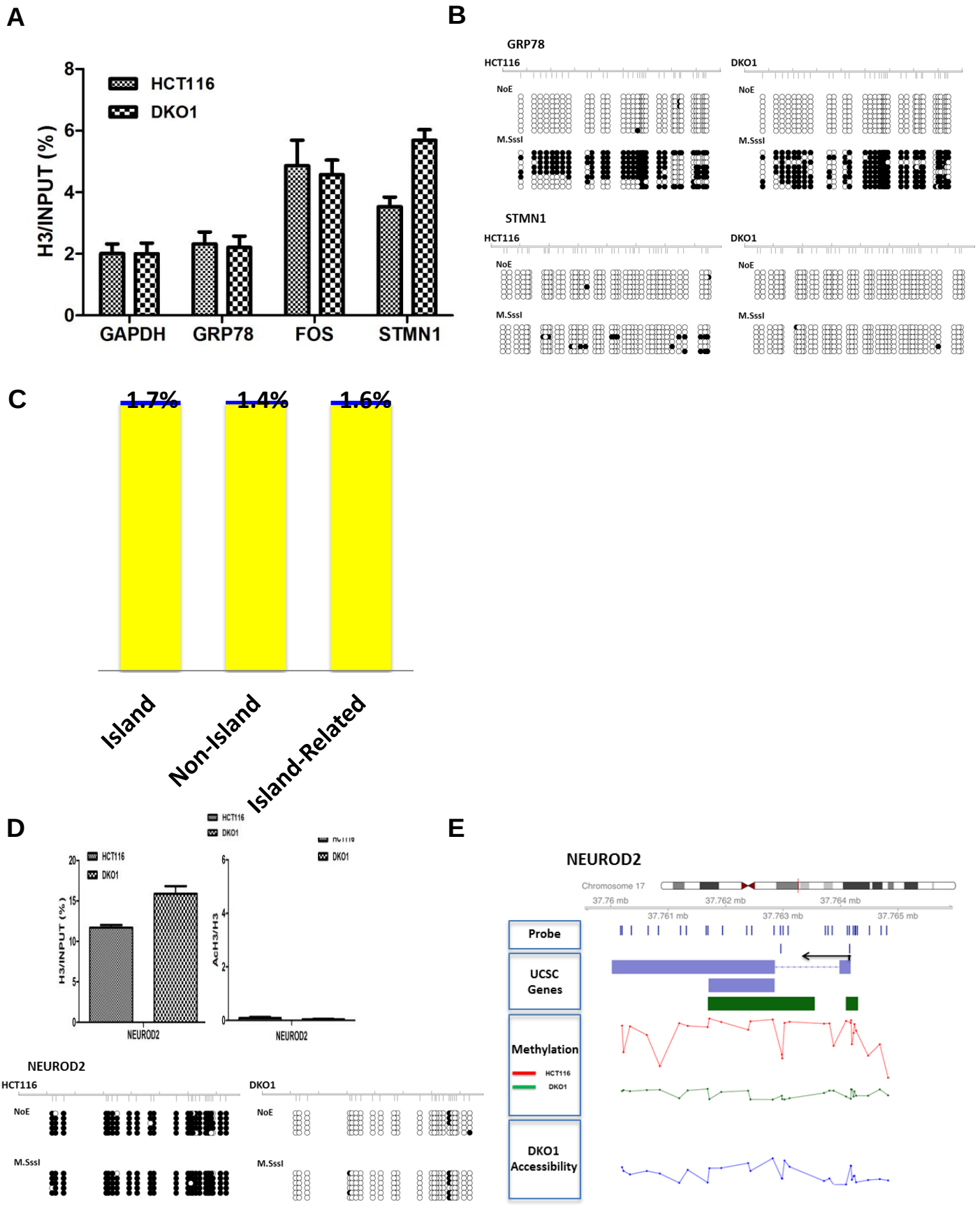

Supplementary Figure 4

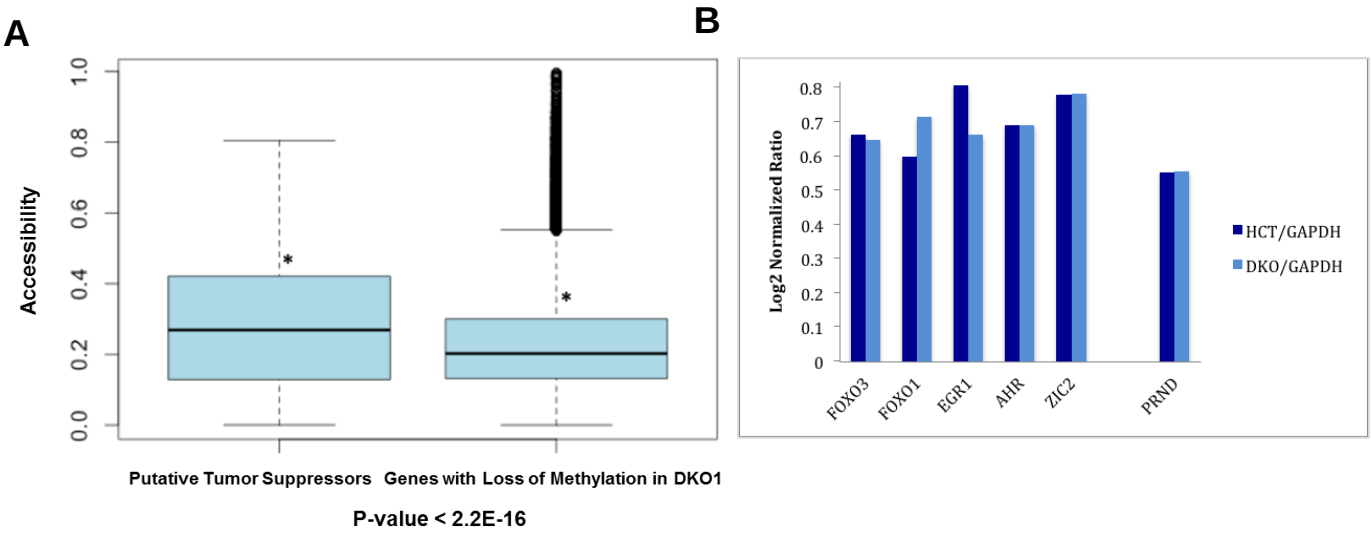

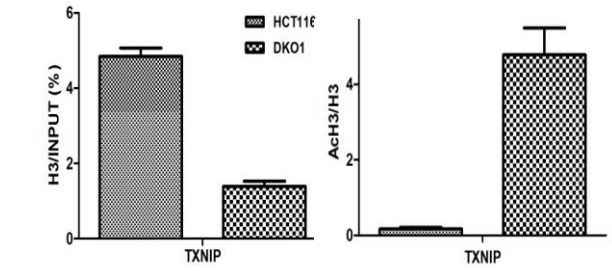

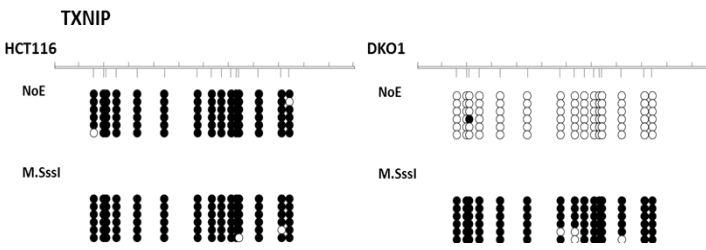

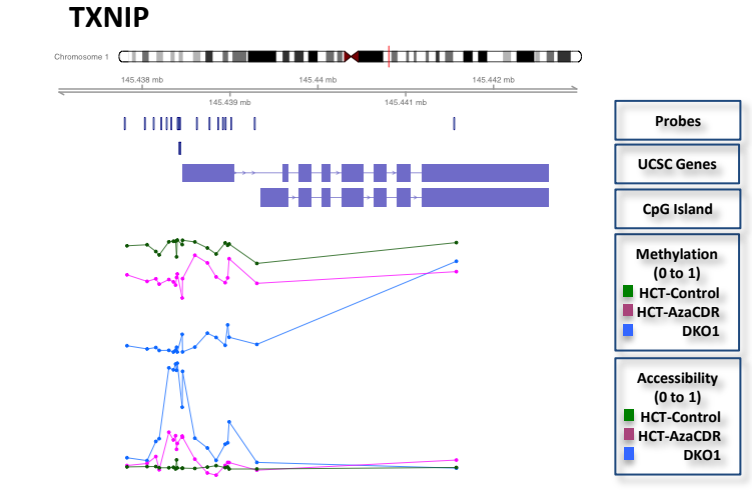

Supplementary Figure 5

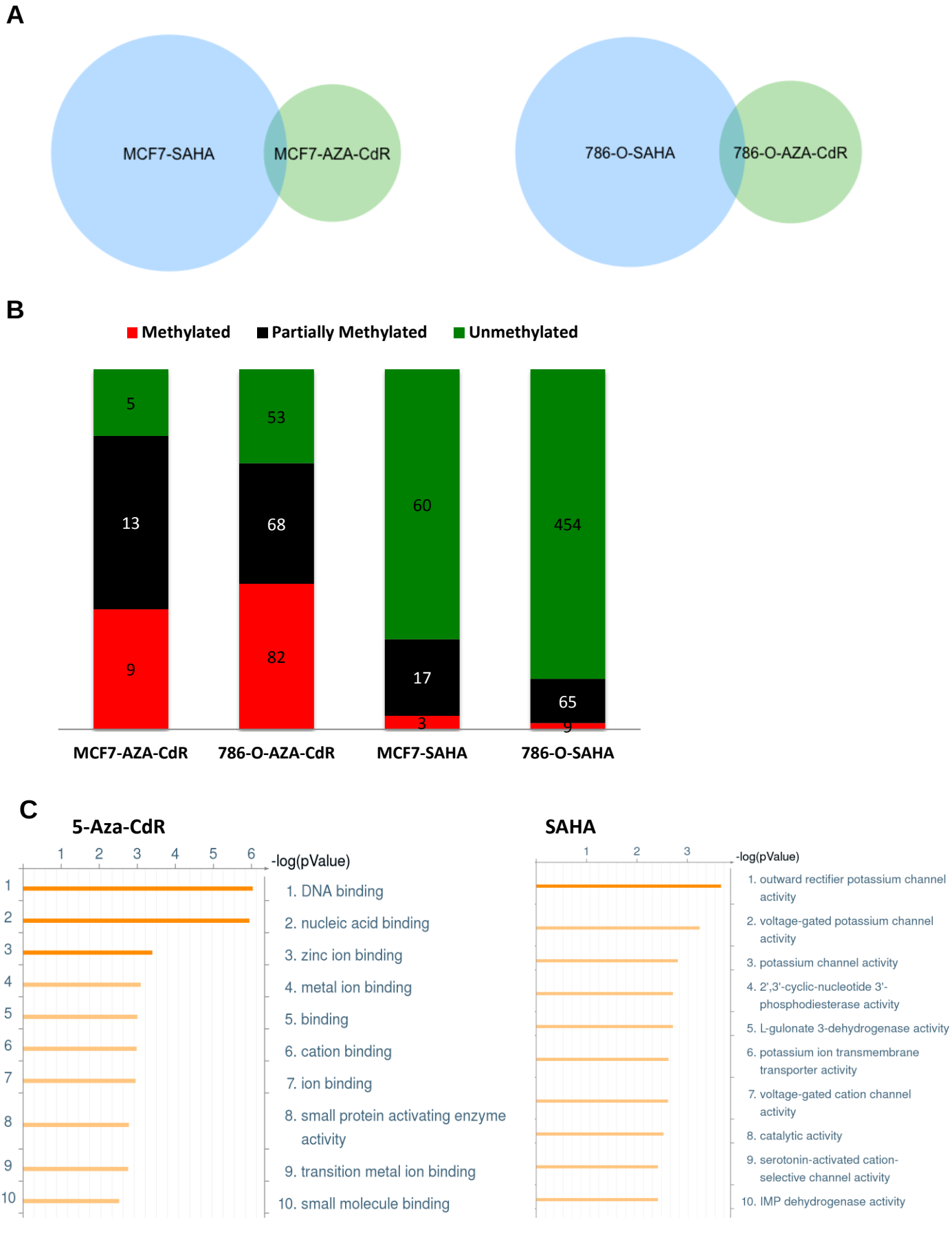

Supplementary Figure 1 (A) Heatmap of all probes for H1 with and without M.SssI treatment (endogenous methylation) shows that, largely, unmethylated regions in H1 gain methylation on M.SssI treatment. (B) ROC analysis was used to determine the optimal cutoff for accessibility, with combined DNAse-seq and FAIRE-seq results as the gold standard. A cutoff of 0.3 had the highest specificity for a sensitivity of greater than 0.5 and, hence, was selected. (C) Regions that are DNAse hypersensitive or FAIRE open, obtained from ENCODE datasets for H1, were determined and accessibility values using Acce*Sss*Ible were obtained for these regions. Venn diagram overlaps show a large degree of overlap between all three methods for H1, with DNAse-seq results having the most number of open chromatin regions. (D) Similar overlaps performed between HCT116 Acce*Sss*Ible data and DNAse data from ENCODE show high degree of overlap between the methods.

Supplementary Figure 2: (A) Density scatter plot comparing accessibilities of HCT116 control and 5-Aza-CdR shows the demethylation that occurs on drug treatment. (B) Kernel density scatter plots of delta-methylation (methylation in treated minus methylation in control) versus delta-accessibility (accessibility in treated minus accessibility in control) for MCF7 (left) and 786-O (right) cell lines show that majority of demethylated loci do not gain accessibility. Groups a and b are events that depict changes in chromatin accessibility independent of DNA methylation while group c depicts regions that gain accessibility upon DNA

demethylation. The scales have been equalized for ease of comparison, with the y-axis ranging from -1 to 1 and the x-axis ranging from -1 to 1.

Supplementary Figure 3: (A) ChIP for histone H3 shows that the genes determined to be open, *GAPDH* and *GRP78*, have a low level of H3 while genes determined to be closed, *FOS* and *STMN1*, have higher levels of H3. (B) Sequencing of the *GRP78* promoter region, determined to be open in both cell lines, and *STMN1* promoter region, determined to be closed in both cell lines, shows a large nucleosome depleted region for *GRP78* and nucleosome occupancy at *STMN1*, corroborating Acce*SssI*ble assay results. (C) Bar graph depicting percentage of demethylated island- (4,743), non-island - (1,603) and island-related, shore, shelf, (3,373) probes in the TSS region that gain accessibility or remain inaccessible upon demethylation. (D) ChIP for H3 shows high levels of histone H3 and low levels of acetylated H3 in both cell lines, indicative of repressed chromatin at the *NEUROD2* promoter. Sequencing results confirm the closed promoter in DKO1. (E) All probes for *NEUROD2* validate the inaccessibility in DKO1 despite a loss of methylation.

Supplementary Figure 4: (A) Comparison of accessibilities of all putative tumor suppressor genes defined by Schuebel et al, 2007, with all genes that lose methylation in DKO1 shows a significant increased accessibility in the first group. (B) Gene expression analysis of transcription factors with enriched binding motifs compared to known negative control *PRND* indicates that the transcription

factors are likely expressed in both HCT116 and DKO1. (C) ChIP for histone H3 and acetylated histone H3 for *TXNIP* shows increased H3 and decreased acetylated-H3 for HCT116, supporting the repressed state, and low levels of H3 and acetylated-H3 for DKO1, supporting that it has attained an open chromatin configuration. (D) Sequencing results validate the determinations in (C). (E) Plot of all probes show a dramatic gain of accessibility in DKO1 and in HCT116 after 5-Aza-CdR treatment right around the transcription start site.

Supplementary Figure 5: (A) Venn diagrams of regions that open in HCT116 and in DKO1 upon 5-Aza-CdR or SAHA treatment show that the drugs have distinct targets in both cells lines. (B) Quantification of the methylation status of probes that gain accessibility upon treatment with 5-Aza-CdR or SAHA shows that 5-Aza-CdR targets regions of methylation whereas SAHA largely targets unmethylated regions. (C) Gene ontology results show enrichment of specific functions in the genes that gain accessibility in HCT116 upon treatment with 5-Aza-CdR or SAHA.